Journal of Metals, Materials and Minerals. Vol. 13 No.2 pp. 53-63, 2004.

THE STUDY OF ISOTHERMAL AND ANISOTHERMAL DEFORMATION BEHAVIORS ON WROUGHT POLYCRYSTALLINE NICKEL BASED SUPERALLOY

Panyawat WANGYAO[1*], Jozef ZRNÍK[2], Ekasit NISARATANAPORN[3], Vladimír VRCHOVINSKÝ[2], and Peter HORŇAK[2]

[1]Metallurgy and Materials Science Research Institute, Chulalongkorn University, Bangkok, Thailand

[2]Materials Science Department, Faculty of Metallurgy, Technical University, Košice, Slovakia

[3]Metallurgical Engineering Department, Engineering Faculty, Chulalongkorn University, Bangkok, Thailand

ABSTRACT

Deformation behavior and damage mechanisms of the wrought polycrystalline nickel based superalloy EI 698 VD has been investigated in different conditions of cyclic creep. At a high temperature of 650°C, isothermal cyclic creep and anisothermal cyclic creep, which were load control with low frequency had been carried out until fracture and was compared to pure creep test. The effect of individual repeating constant tensile load holding time (1, 3, and 10 hr.) superimposed during creep at a stress level of 740 MPa in both cyclic creep tests were studied. The influence of holding time was evaluated through the deformation behavior (strain to fracture) and strain rate, lifetime, and fracture mechanisms participating in failure process through microstructure, crack nucleation and propagation of fractured specimens. The results can be concluded that the time to fracture increased in case of isothermal cyclic creep comparing to creep lifetime. However, in the case of the anisothermal cyclic creep, lifetime increased as holding time decreased. The effect of fatigue component participating in fracture mechanism just appeared slightly only in the latter cyclic creep, which had the shortest holding time (1 hr.).

Keywords: Isothermal, Anisothermal, Deformation, Cyclic Creep, Nickel based superalloy

* To whom correspondence should be addressed:
E-mail: panyawat@hotmail.com Tel: (662) 218 4233 Fax : (662) 611 7586

INTRODUCTION

EI 698 VD, one of many grades of polycrystalline gamma prime-strengthening nickel base superalloy, exhibiting superior high-temperature strength properties, is nowadays commonly used in Russian and former Eastern European countries for both military and commercial aircraft, and power plant industries for advanced turbine engines as shafts and discs. The alloy is a well-known material due to its excellent mechanical properties such as high resistance to plastic deformation (tensile, creep and fatigue), structural stability, corrosion and oxidation resistance at high temperature for aircraft gas turbine engine. These favorable properties result mainly from complex structures consisting of a coherent gamma prime precipitating phase in gamma matrix and carbides precipitates at grain boundaries (Decker, *et al.* 1972; Betteridge, *et al.* 1977; Betteridge, *et al.* 1974; and Donachie, 1984).

In the vast majority of aero applications, the various components are subjected to repeated thermal and mechanical loading, thus making high temperature cyclic deformation and failure a primary concern for long-term structural integrity and component life. Therefore, high temperature creep strength and thermomechanical fatigue (TMF) resistance are considered to be the major concern of mechanical properties .

While several detailed studies on the high temperature creep behavior of nickel based superalloy have been performed in the past (Donachie, 1984; and Tien, *et al.* 1989). Much less works have been carried out in the isothermal and, in particular, on anisothermal thermomechanical cyclic creep of the alloys. The understanding of the isothermal cyclic creep behavior can provide a useful basic guideline and knowledge to anisothermal or thermomechanical cyclic creep. Anyhow, by itself, it is still insufficient to deal with the latter, which is a much more complicated deformation process.

The effect of cyclic loading, in general, can either accelerate or decelerate creep rate depending on stress, temperature conditions and microstructure characteristics of materials (Tien and Caulfield, 1989). The creep acceleration effect in nickel based superalloys can be attributed to different mechanisms involving anelastic strain storage and recovery, carbide precipitation, effect of primary creep repeating, and recovery and work hardening during steady-state creep during on-load hold time (Tien, *et al.* 1989; Zrnik, *et al.* 1997; Wangyao, *et al.* 1997; and Zrnik, *et al.* 2000). The goal of the present work is to gain a deeper exact understanding of the influence of the additional fatigue stress component superimposed onto the creep test for both isothermal and anisothermal (thermomechanical) cyclic creep on deformation behavior, lifetime and fracture mechanism in EI 698 VD.

MATERIALS AND EXPERIMENTAL PROCEDURE

The investigated material was wrought polycrystalline EI 698 VD, one of the precipitate strengthening nickel based superalloys developed in the Russian aircraft industry. The superalloy is used for turbine shafts and discs. Chemical composition of the superalloy in wt. % is shown in Table 1. To obtain the required mechanical properties at room and elevated temperatures, three step heat treatment was done:

1) Solution annealing at 1,100°C for 8 hours then air cooling

2) Ageing at 1,000°C for 4 hours then air cooling

3) Ageing at 775°C for 16 hours then air cooling

Table 1 Chemical composition (wt. %) of EI 698 VD.

Ni	Cr	Mo	Ti	Nb	Fe	Al	C	Si	Mn	P	S
Bal.	13-16	2.8-3.2	2.3-2.7	1.8-2.2	Max. 2.0	1.3-1.7	0.08	Max. 0.6	Max. 0.4	Max. 0.015	Max. 0.007

Uniform gauge section specimens with a diameter of 0.5 mm. were machined for all types of testing. The pure creep, isothermal and anisothermal cyclic creep tests had been carried out in creep testing machines allowing the applied load to remain constant during testing. The test conditions for individual testing were as following:

1) Creep tests were done under stress of 740 MPa and at a temperature of 650°C until fracture.

2) The load wave diagram (Figure 1) for isothermal cyclic creep as a function of time was a trapezoidal shape and unchanged until rupture. Constant peak load at three different holding times of 1, 3, and 10 hours were carried out. The rise and fall time was 1 minute. The stress after load reduction was maintained at R = 20 MPa to keep the loading system in tension. The testing temperature for isothermal cyclic creep test was 650°C and kept constant during testing.

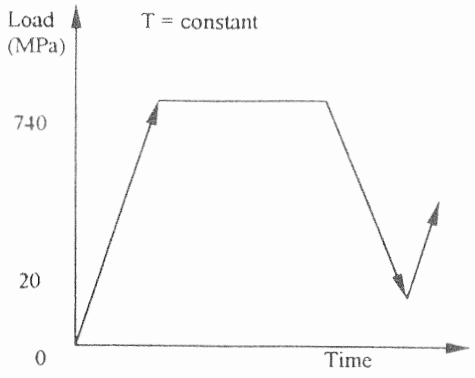

Figure 1 Isothermal cyclic creep waveform.

3) The anisothermal cyclic creep loading schedule and testing conditions were the same as those for isothermal cyclic creep testing, the only temperature change was introduced into load waveform by air cooling the specimens prior to each load reduction and reheating prior to each reloading, see load wave diagram in Figure 2.

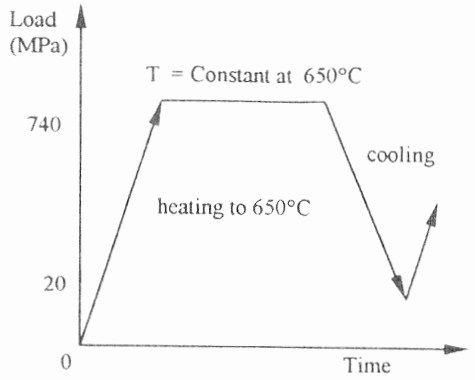

Figure 2 Anisothermal cyclic creep waveform.

It should be noted that all tests had been carried out until the specimens fractured. The tests were characterized by strain, strain rate, and lifetime. The thin foil samples for TEM observation were prepared from the gauge sections of fractured specimens. These samples were mechanically thinned, followed by electrolytic thinning and examined in TEM operating at 200 kV. A TEM analysis was used to reveal a dislocation structure and dislocation deformation mechanisms for applied testing procedure.

Metallography examinations were carried out in a plane parallel to the test piece axis. These examinations permitted to relate more closely to the crack propagation path to specimen structure. Fracture surfaces of all test pieces were systemically examined by SEM to determine the fracture mode and specific characteristics of fractures because of the fatigue stress component introduction onto creep stress.

RESULTS AND DISCUSSION

Mechanical Testing

Isothermal Cyclic Creep

Figure 3 shows the strain-lifetime curve for the cyclic creep tests with applied stress R = 740 MPa and different holding time at maximum stress level. The strain-time curve shows that the introduction of cyclic creep component superposition in static creep resulted in a positive change of the lifetime until fracture. Isothermal cyclic creep results are slightly scattering, however, it can be overall suggested that the number of unloading affected cyclic creep by increasing lifetime and increasing minimum strain rate comparing to pure creep, see Table 2. From previous theories in cyclic creep at low frequency, it is well known that there is general behavior, which load relaxing can accelerate minimum strain rate resulted in the increase of rupture strain and decreasing lifetime.

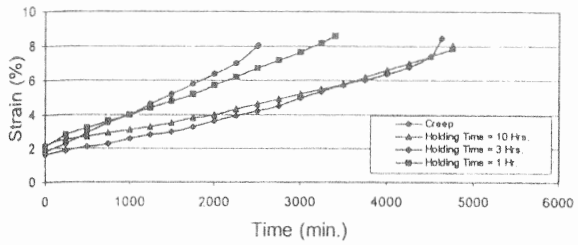

Figure 3 Strain-Lifetime curve of Isothermal Cyclic Creep.

The basic explanation for such effect is that during the off load period (load relaxing), the hardened dislocation substructure formed during the on load period recovering in off-load periods (Tien, *et al.* 1989; Zrnik, *et al.* 1997; Wangyao, *et al.* 1997; Zrnik, *et al.* 2000; and Zrnik, *et al.* 2003). Thus when load repeated, a period of primary creep occurring again until work hardening resulted in the steady-state creep rate observed during the static creep in each cycle. These repeated periods of primary creep during the initial portion of the on-load cycle cause the creep acceleration.

However, the above explanation is not completely proper to the results of the present work. According to the results, it can be suggested that during the tests there was a complex competition between: 1) effect of repeated periods of primary creep, which could increase rupture strain and minimum strain rate; 2) effect of off-load and on-load cycles caused deformation undergoing in different slip planes. In such way, dislocations did not move continuously in the same slip planes as those during static creep. They were forced to change direction of moving and so they could meet new obstacles in other directions (such as precipitating gamma prime, carbides and other dislocations). The latter effect might prolong the cyclic creep lifetime and decrease minimum strain rate.

Table 2 Results of Isothermal Cyclic Creep.

Holding time (hr.)	Fracture strain (%)	Total creep lifetime (min)	True elongation (%)	Approximated lifetime at true elongation (min)	Minimum strain rate (%/min)
0 (creep)	7.96	2,512	**6.35**	**2,000**	2.396×10^{-3}
10	8.055	4,755	**4.16**	**2,500**	2.401×10^{-2}
3	8.471	4,625	**4.58**	**2,400**	2.902×10^{-2}
1	9.064	3,406	**6.23**	**2,100**	4.314×10^{-2}

Anisothermal Cyclic Creep

Different trends in deformation behavior were observed in the type of cyclic creep where the change of temperature was introduced into the deformation cycle. The results of this cyclic creep are shown in Figure 4. It was found that the effect of number of off-load with temperature reduction provided a lower fracture strain and minimum

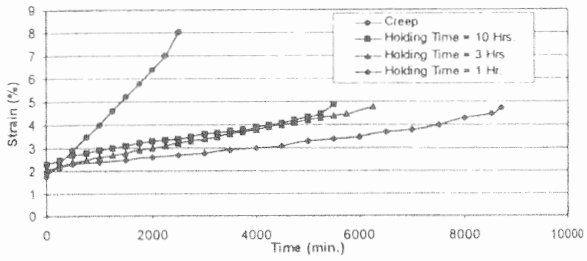

Figure 4 Strain-Lifetime curve of Anisothermal Cyclic Creep.

strain rate, and a longer lifetime comparing to the first program. The strengthening effect became more pronounced as frequency of cycling increased. In addition, during off-load periods at room temperature after cooling by air there was not any effect of recovery process. Dislocation density was still reserved. Thus, the substructure was also still in a deformed or hardened state. When reloading again with increasing temperature, such hardened substructure should result in a very low effect of primary creep repetition. However, it still resulted in a bit faster minimum strain rate than that in the case of pure creep. The strengthening was also slightly obtained because of dispersive deformation in different slip planes during loading. Thus, this should provide the lower fracture strain, minimum strain rate, and longer lifetime.

However, it was also possible to measure ductility in two ways; which is ductility of true elongation (elongation at the finishing point of secondary creep period) and total elongation (fracture strain, already discussed above). From previous knowledge (Reed-Hill and Abbaschain 1994), total elongation of metals under rupture stress tests (same method as creep test but has to be done until fracture at applied high stress levels) is usually scattering and not enough reliable. Total elongation may be higher or lower even though they have the same testing conditions. It is due to the effect of quantity of cracks and crack dispersion during tertiary creep. Crack propagation has a slightly higher effect on rupture time but has a greater influence on total elongation. Thus, it has been believed that true elongation will provide a more accurate representation of ductility than total elongation. From data in Tables 2 and 3, it can be approximately concluded that total lifetime decreased as rupture time increased (Figure 5a) and true elongation values decreased as rupture time increased (Figure 5b and 5c) which is similar to pure creep tests. It should be also noted that the points in Figure 5b are average closer to the curve than those of Figure 5a.

Table 3 Results of Anisothermal Cyclic Creep.

Holding time (hr.)	Fracture strain (%)	Total creep lifetime (min)	True elongation (%)	Approximated lifetime at true elongation (min)	Minimum strain rate (%/min)
0 (creep)	7.96	2,512	**6.35**	**2,000**	2.396×10^{-3}
10	6.835	3,444	**3.85**	**3,000**	4.175×10^{-3}
3	6.677	4,236	**3.79**	**3,600**	3.684×10^{-3}
1	4.78	7,910	**3.43**	**5,000**	2.369×10^{-3}

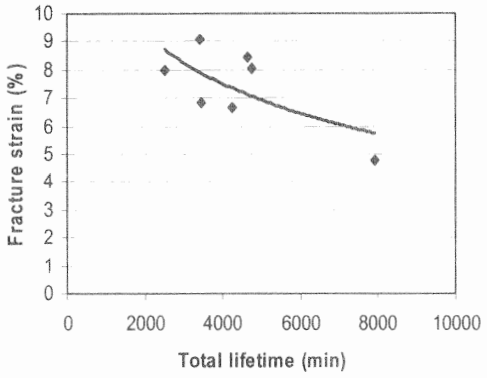

Figure 5a The relationship between total lifetime and fracture strain for both isothermal and anisothermal cyclic creep.

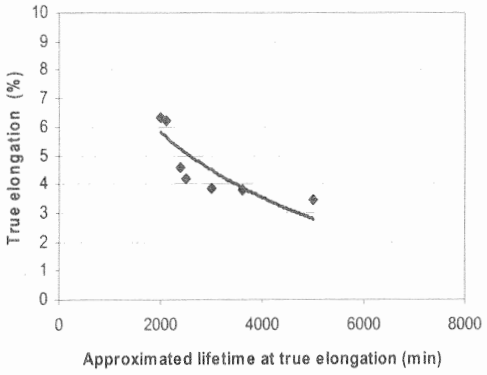

Figure 5b The relationship between approximated lifetime at true elongation and true elongation for both isothermal and anisothermal cyclic creep.

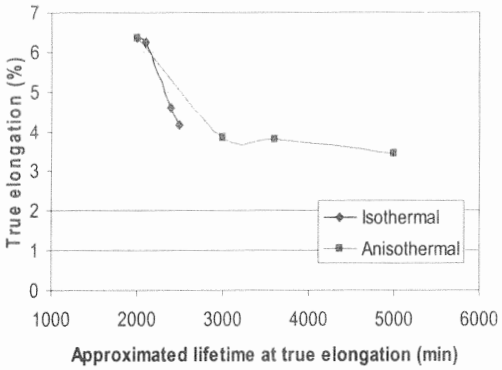

Figure 5c The more detailed relationship between approximated lifetime at true elongation and true elongation for both isothermal and anisothermal cyclic creep.

MICROSTRUCTURE STUDIES

Prior Microstructure

The heat treatment procedure provided a uniform equiaxed grain microstructure. Coarse, bulky, MC carbides, which are a result of eutectic reaction, were deposited inside of grains and along grain boundaries, Figure 6. Ageing at higher temperature has also led to precipitation of $M_{23}C_6$, chromium based carbides of a finer size at intergranular locations, Figure 7. Two-steps ageing treatment resulted in over 40% volume fraction of gamma prime precipitates and these were uniformly distributed in the gamma matrix. Bright field TEM micrograph presents these precipitates in Figure 8. The gamma prime is intermetallic phase $Ni_3(Al, Ti)$ with face-centered cubic structure ($L1_2$). It is coherent with a matrix and has either a cuboidal or globular morphology. The sphere shaped gamma prime precipitates are about 40 to 80 nm in diameter. In a temperature range of 650-900°C, they are very stable and provide excellent high temperature strength and creep properties.

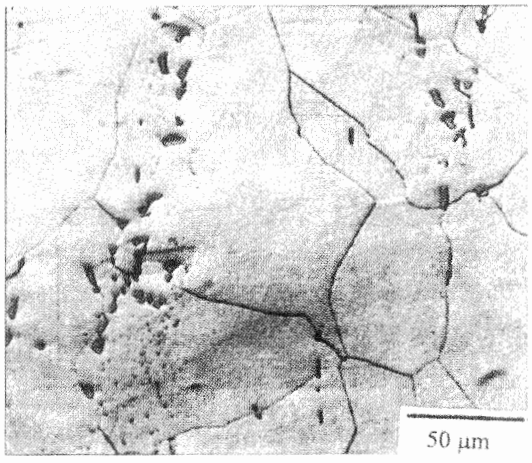

Figure 6 Microstructure of the alloy after heat treatment.

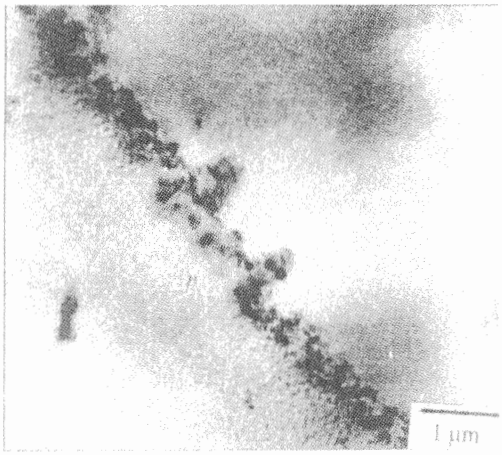

Figure 7 TEM micrograph of $M_{23}C_6$ carbides on grain boundary.

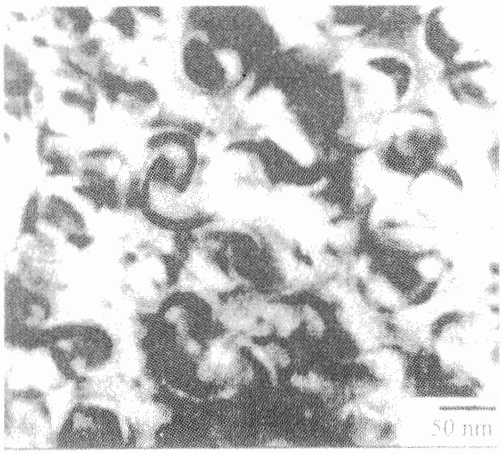

Figure 8 TEM micrograph of gamma prime precipitate.

Substructure of deformation processes

An extensive TEM analysis was carried out to study the post deformation dislocation structure developed in deformed or fractured specimens due to different regimes of loading. The principal aim of this analysis was to assess the effect of both isothermal and anisothermal cyclic creeps on the deformation behavior of the alloy.

In case of pure creep of 1hr duration, within this short period of transient creep deformation, planar dislocation arrangements (slip bands) were developed, Figure 9. However, a homogeneous dislocation network within the slip bands was already observed. Dislocation-particle interactions were noticed also in the matrix between slip bands. The dislocation configurations provide the evidence, which dislocation Orowan bowing and particle shearing participated in dislocation surpassing the gamma prime precipitates. An evidence of particle shearing by glide dislocations in slip band is presented in Figure 10 and Orowan bowing is shown in Figure 11.

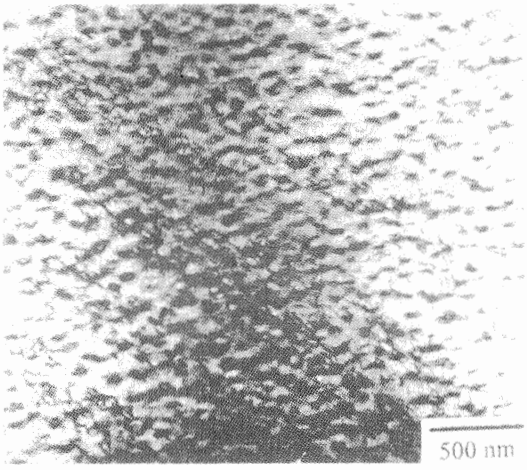

Figure 9 Planar slip band in crept specimen after 1 hr-creep test.

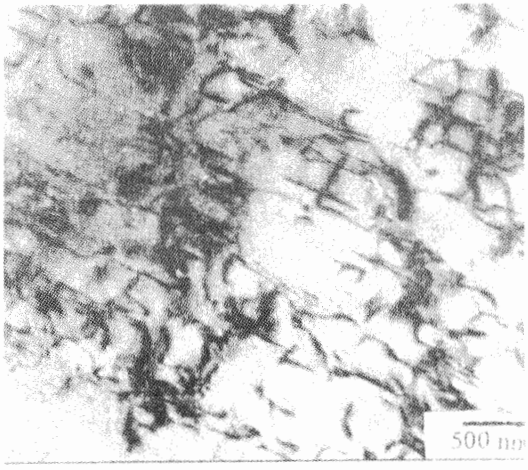

Figure 10 Particle shearing within slip band, creep 1 hr.

As creep duration exceeded 25 hours the dense dislocation arrangements were more developed, Figure 12. In this case, the

precipitates were circumvented by the Orowan looping process or dislocation passed over the gamma prime precipitates by the climbing process, as shown in Figure 13.

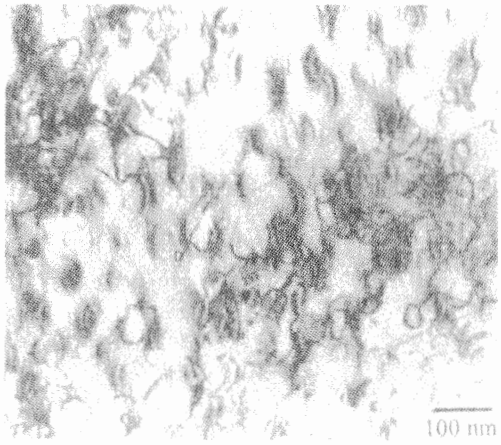

Figure 11 Orowan bowing of dislocation.

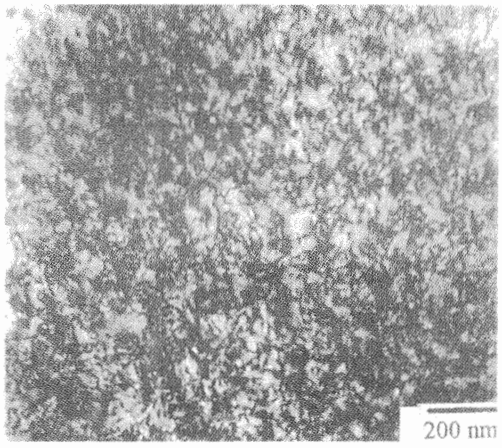

Figure 12 Dislocation tangles in matrix, creep 25 hr.

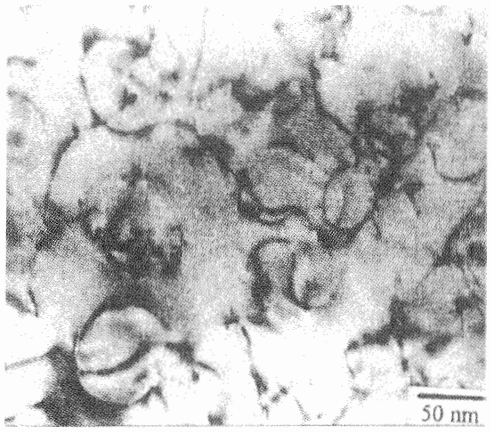

Figure 13 Dislocation climbing in matrix.

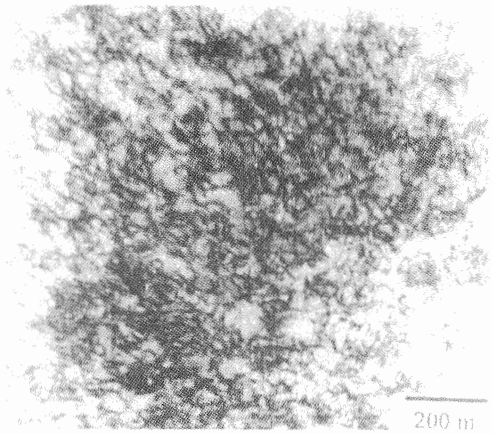

Figure 14 Dense dislocation tangles in matrix.

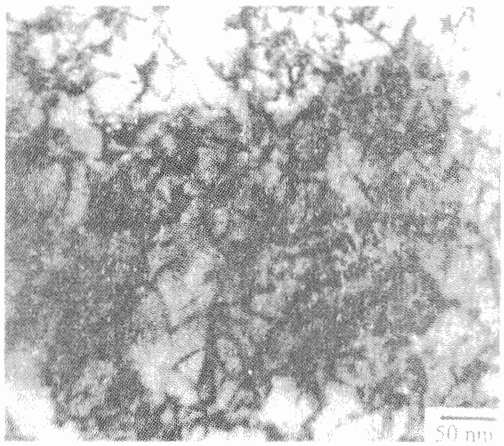

Figure 15 Dislocation clusters built up at precipitates.

The dislocation substructure corresponding to the fractured specimen is presented in Figure 14. The dislocation tangles as clustered around the precipitates are shown in Figure 15. The gamma prime precipitates remained uniformly distributed and did not change morphologically during creep.

The deformation in the specimens subjected to isothermal cyclic creep was studied only in the fractures part of the specimen. Regardless of the individual cyclic test variables (different holding times), the dislocation close to fracture bears the features of severe plastic deformation, identical to only crept specimens. Homogeneous distribution of dislocations was noticed in intragranular areas. However, in gauge length, more remote from fracture surface, where dislocation network

was less dense the shearing of gamma prime precipitates and dislocation clustering due to interaction with precipitates were observed as well.

TEM structure analysis of specimens, which were tested under cyclic creep with temperature change according to the applied load reveled no substantial changes in developing of dislocation substructure. In spite of apparent specimen, hardening at all tests, and comparing with creep test, the dislocation substructure in fractured specimens did not differ from those observed under the monotonic creep test, Figure 16. Orowan bowing dislocation mechanisms, no matter holding time, was dominant for anisothermal deformation, Figure 17.

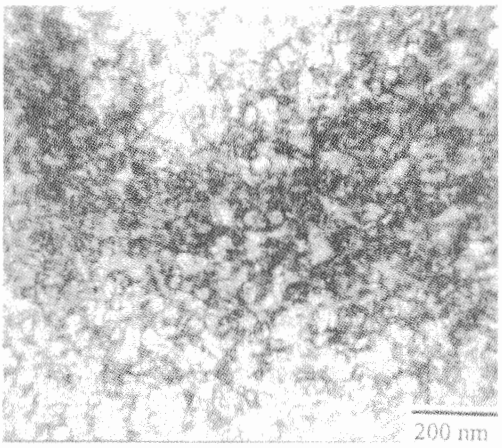

Figure 16 Dislocation configuration in specimen under anisothermal cyclic creep test.

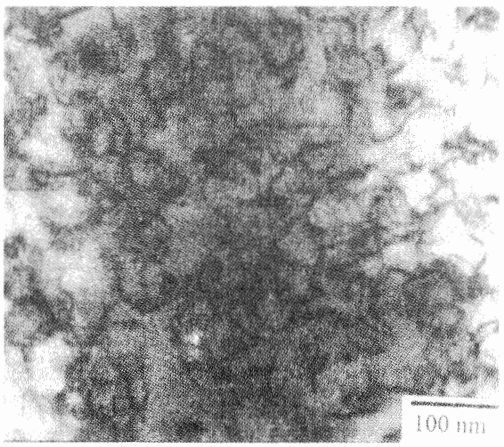

Figure 17 Dislocation bowing surpassing precipitates.

To conclude the obtained TEM results, the investigation of the deformation process indicates, regardless of individual choice of testing schedules, that introduction of a cyclic stress component of defined parameters onto creep stress resulted only in the amount of deformation work and extension of time to fracture. Creep/fatigue deformation did not affect obviously the dislocation mechanism participating in deformation. The shearing of gamma prime precipitates within matrix could occur because of the extensive work hardening in slip bands. It appeared that the increased internal resistance due to dislocation tangling within slip bands is much larger than the stress required for initiating the shearing of gamma prime precipitates in the inter slip band areas. However, it seems to be evidenced that with prevailing cycling stress, mainly in the initial stage of test, the deformation was more inhomogeneous and condensed in more narrow slip bands. In this case gamma prime precipitates shearing in slip bands, sets up preferential paths for the movement of dislocations in the early stage of deformation.

DAMAGE MECHANISMS

The SEM fracture analysis of broken specimens was employed to trace the crack initiation site and its morphology, as well as the fracture mode, with consideration of microstructure. Metallography examination along a plane normal to the crack propagation showed that crack path has a mixed intergranular and transgranular character. Nevertheless, secondary cracks, which were few on cross section, nucleated on grain boundaries with perpendicular orientation to applied stress and had either wedge or flat morphology. Fracture initiation was always, regardless of testing type, found at specimen surface. In both creep and isothermal cyclic creep tests, all fractured had characteristic intergranular crack initiation and propagation, as shown in Figure 18. Only the total intergranular area differed for relating individual testing. After critical crack opening, its further propagation was mixed fracture

mode, intergranular and transgranular cleavage, Figure 19. The only fatigue stress participation at crack nucleation process was observed in anisothermal cyclic creep of one-hour holding time, and of pure fatigue testing, Figure 20. However, the resulting fracture mechanisms for further crack propagation were identical to other fractures.

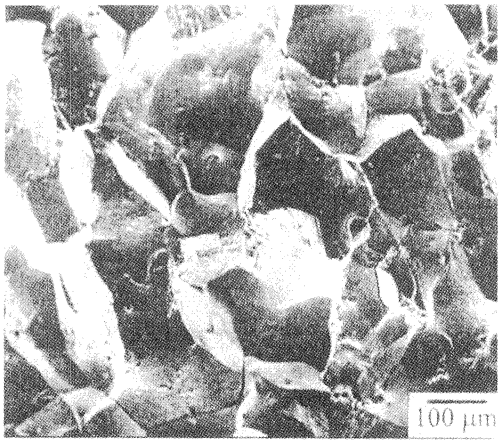

Figure 18 SEM micrograph of fracture surface, crack initiation.

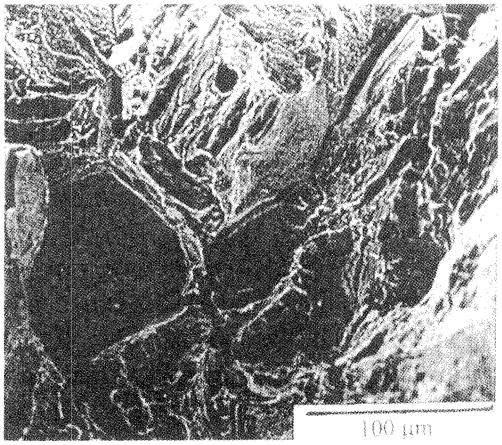

Figure 19 SEM micrograph of intergranular and transgranular cleavage.

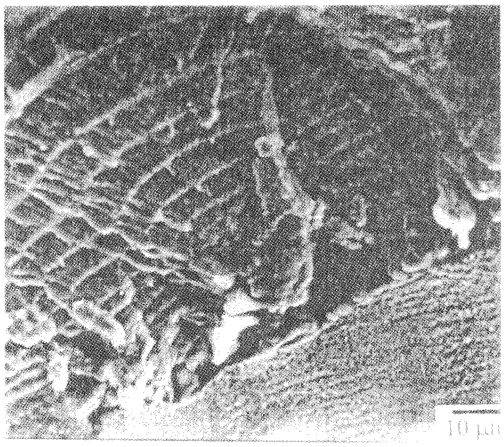

Figure 20 Fatigue mechanisms crack initiation in specimen of 1 hr hold time of anisothermal cyclic creep.

CONCLUSION

The mechanisms of deformation and damage at high temperature in wrought nickel based superalloy EI 698 VD were investigated under creep, isothermal and anisothermal cyclic creep tests. The TEM and SEM experimental techniques were employed for analysis of dislocation structure and fracture process. The following conclusions can be drawn from the present study:

1) In both cyclic creep conditions, load relaxing could cause slightly positively an increase in fracture lifetimes.

2) Fracture lifetimes from anisothermal cyclic creep are longer than those from isothermal cyclic creep tests at the same duration. This might be due to the hardened microstructure after each on-load period of anisothermal cyclic creep was not eliminated by the recovery process as that in the isothermal cyclic creep.

3) The detrimental effect of the creep process is much less pronounced when shorter on-load periods were performed in the case of anisothermal cyclic creep.

4) The shorter on-load period provided the longer lifetime at true elongation in case of cyclic creep with temperature change.

5) True elongation generally decreases with the increase of rupture lifetime.

6) At initial stages of each applied loading schedule, the deformation is localized into planar slip bands. The width of slip bands seemed to depend on loading schedule.

7) Shearing of gamma prime precipitates in slip bands were found in a preferential path for dislocation movement for pure creep loading.

8) More advanced testing promotes development of dense dislocation network in gamma matrix. The dislocation formed dense clusters around precipitates.

9) Orowan bowing and dislocation climbing mechanisms are to surpass the precipitates when deformation preceded at all applied loading regimes.

10) The intergranular crack initiation and propagation had a uniform mechanism for all types of testing. Only for shortest hold time of anisothermal cyclic creep test, the creep/fatigue interaction was appeared with characteristic fatigue striations at crack initiation.

REFERENCES

Betteridge, W. 1977. *Nickel and its Alloys*. New York, Macdonal and Evans.

Betteridge, W. and Heslop, J. 1974. *The Nimonic Alloys and other Nickel Base High Temperature Alloys*. 2nd ed. New York, Crane, Russak & Co.

Decker, R. F. and Sims, C. T. 1972. *The metallurgy of nickel base alloys in the superalloys*. New York, John Wiley & Son Inc.

Donachie, M. J. Jr. 1984. *Superalloys Source Book*. Metals Park, Ohio. American Society for Metals.

Reed-Hill, R. E. and Abbaschain, R. 1994. *Physical Metallurgy Principles*. 3rd ed. Boston. PWS PUB.

Tien, J. K. and Caulfield, T. 1989. *Superalloys, Supercomposites and Superceramics*. Boston. Academic press.

Wangyao, P., Nisaratanaporn, E., Zrnik, J., Vrchovinsky, V. and Hornak, P. 1997 High temperature properties of wrought nickel base superalloy in creep-fatigue conditions. *J. Met. Mater. Miner.* **7**(1) : 1-12.

Zrnik, J. and Wangyao, P. 2000. Microstructural study of nickel base superalloy subjected to creep, isothermal cyclic creep and thermomechanical fatigue, *J. Acta Metall. Slovaka*. **3** : 233-241.

Zrnik, J., Semenak, J., Wangyao, P., Vrchovinsky, V. and Hornak, P. 2003. Analysis of low cycle fatigue behavior in nickel base superalloy, *J. Met. Mater. Miner.* **12 (2)** : 33-40.

Zrnik, J., Wangyao, P., Vrchovinsky, V., Hornak, P. and Mamuzic, I. 1997. Deformation behaviour of wrought nickel base superalloy in conditions of thermomechanical fatigue. *J. Metall.* **(4)** : 225-228.

(Revised version accepted March 17, 2004)